Reaction Kinetics, Mechanisms and Catalysis (2018) 125:1–13
https://doi.org/10.1007/s11144-018-1435-8

Analytical solution of the Langmuir-based linear driving force model and its application to the adsorption kinetics of boscalid onto granular activated carbon

Angelo Fenti[1] · **Stefano Salvestrini**[1,2]

Received: 18 May 2018 / Accepted: 14 June 2018 / Published online: 19 June 2018

Abstract

The application of intraparticle diffusion models is generally difficult because of complex mathematical structure. The linear driving force (*LDF*) approach reduces the mathematical effort and provides a reasonable approximation of the intraparticle diffusion theory. In this work, an exact analytical solution of a *LDF* equation based on the Langmuir equilibrium model (*LLDF*) was derived. The *LLDF* model depends on three unknown parameters, namely the adsorbed amount at equilibrium, the maximum adsorbent capacity and the mass transfer coefficient. The *LLDF* model was used for analyzing the adsorption kinetics of boscalid onto granular activated carbon. The experimental results at equilibrium showed that the maximum adsorption capacity of activated carbon for boscalid and the Langmuir equilibrium constant of the process were 167 mg g^{-1} and 0.53 L mg^{-1}, respectively. The *LLDF* equation was successfully applied to the kinetic data, allowing the evaluation of the mass transfer coefficient of boscalid (8.4×10^{-3} h^{-1}). The *LLDF* model has general validity for describing intraparticle diffusion-adsorption onto porous media and its reliability can be assessed by a simple graphical method.

Keywords Linear driving force · Intraparticle diffusion · Langmuir isotherm · Boscalid · Adsorption · Adsorption kinetics

✉ Stefano Salvestrini
stefano.salvestrini@unicampania.it

[1] Department of Environmental, Biological and Pharmaceutical Sciences and Technologies, Università degli Studi della Campania Luigi Vanvitelli, Via Vivaldi 43, 81100 Caserta, Italy

[2] Environmental Technologies srl, University Spin-off, Università degli Studi della Campania Luigi Vanvitelli, via Vivaldi 43, 81100 Caserta, Italy

Introduction

Adsorption has a central role in a diversity of natural processes ranging from molecular interaction in biological systems [1, 2] to the dynamics of pollutants in water/soil systems [3–6].

Adsorption-based methods are largely applied in the field of water decontamination because of their efficiency, ease of use and low cost compared to other procedures [7–10].

A comprehensive characterization of an adsorption process requires information not only on the thermodynamics (especially on equilibrium conditions) but also on the kinetics of the process. Notably, most adsorbents are porous media and this may have a relevant effect on the adsorption kinetics since the rate of the process is generally limited by the ability of adsorbable molecules to diffuse into the interior of the adsorbent through the pores.

It is commonly agreed that diffusion-adsorption in a porous medium proceeds through four consecutive steps [11]: (i) transport of the solute from the bulk phase to the boundary layer around the adsorbent particle; (ii) diffusion of the solute from the boundary layer to the external surface of the adsorbent (film diffusion); (iii) diffusion of the solute through the pores to the immediate vicinity of the internal adsorption surface (pore diffusion or intraparticle diffusion); (iv) adsorption onto the adsorbent site. Steps (ii) and (iii) are generally the rate-limiting steps of the overall process [12].

Basic equations of diffusion were first derived by Fick, who exploited the analogy between diffusion and heat conduction [13]. Fick's first law states that the flux J of the diffusing substance is proportional to the concentration gradient $\partial C/\partial x$ [14]:

$$J = -D\frac{\partial C}{\partial x} \tag{1}$$

Here the flux J is defined as the amount of substance diffusing along the space coordinate x through a unit area normal to x, during the unit time t; C is the substance concentration and D its diffusion coefficient.

Equation 1 can be used to derive the Fick's second law, which gives the time dependence of C at a given position x:

$$\frac{\partial C}{\partial t} = D\frac{\partial^2 C}{\partial x^2} \tag{2}$$

Equation 2 applies if the concentration varies only along one dimension (x, in our case) and D is assumed independent of concentration.

If we restrict ourselves to the diffusion in a sphere (i.e. radial diffusion), we can express the diffusion rate in terms of polar coordinates, so that Eq. 2 turns into:

$$\frac{\partial C}{\partial t} = D\left(\frac{\partial^2 C}{\partial \sigma^2} + \frac{2}{\sigma}\frac{\partial C}{\partial \sigma}\right) \tag{3}$$

Here σ is the radial distance from the center of the sphere.

By integrating Eq. 3, the amount of diffusing substance (M) entering or leaving the sphere at time t and ∞ [15] is:

$$\frac{M_t}{M_\infty} = 1 - \frac{6}{\pi^2}\sum_{n=1}^{\infty}\frac{1}{n^2}\exp\left(-\frac{Dn^2\pi^2 t}{r^2}\right) \tag{4}$$

Here r is the radius of the sphere.

Based on the above considerations, in a system where the adsorption rate is governed by pore diffusion and assuming that the adsorbent particles are spherical we may rewrite Eq. 4 as:

$$\frac{q}{q_e} = 1 - \frac{6}{\pi^2}\sum_{n=1}^{\infty}\frac{1}{n^2}\exp\left(-\frac{Dn^2\pi^2 t}{r^2}\right) \tag{5}$$

Here M_t and M_∞ have been replaced with the adsorbed amount at time t (q) and at equilibrium (q_e), respectively.

A great deal of effort have been directed at deriving an approximated form of Eq. 5 easily applicable to the experimental data for ascertaining whether the adsorption process is diffusion-controlled. A simplified pore diffusion model (see Eq. 6) was derived from Eq. 5 by [15] for the reaction still far from equilibrium:

$$\frac{q}{q_e} = \frac{6}{\sqrt{\pi}}\sqrt{\left(\frac{Dt}{r^2}\right)} \tag{6}$$

Equation 6 was later slightly modified by Weber and Morris [16] and thereafter extensively used for modelling adsorption kinetic data [17–21].

According to Eq. 6, when pore diffusion dominates, a linear relationship between q and $\sqrt{t}$ should be observed in the early stage of the experiment; in that case, D could be calculated from the slope of the line. It is worth noting that this method is sensitive to the lack of experimental data in the initial phase of reaction and/or the use of too large an acquisition time, possibly leading to an incorrect measure of D and/or a misleading interpretation of the results, especially for fast reactions.

An alternative way for interpreting the adsorption kinetics of pore diffusion-controlled processes is the surface diffusion approach [22], according to which the mass transfer occurs in the *adsorbed state*. In this view, the adsorbate gradient is the driving force for the mass transfer and therefore the flux J can be expressed in terms of q by the following equation:

$$J = \rho_S D_s \frac{\partial q}{\partial \sigma} \tag{7}$$

Here ρ_S is the particle density and D_s the surface diffusion coefficient.

Equation 7 can be substantially simplified by assuming the solid-phase concentration gradient to be linear, as in the so-called linear driving force (*LDF*) model [23]. In so doing, Eq. 7 reduces to:

$$J =_S k_S(q_S - q) \tag{8}$$

$$k_S = \frac{D_S}{r} \tag{9}$$

Here q_S is the adsorbed amount at the outer surface of the adsorbent particle in equilibrium with the bulk solution concentration at time t, q is the *mean* adsorbed amount inside the particle at the same time, whereas the diffusional parameter k_s is defined as in Eq. 9. Moreover, by applying the mass conservation principle, we obtain:

$$J = -\frac{V_L}{A_S}\frac{dc}{dt} = \frac{m_A}{A_S}\frac{dq}{dt} \tag{10}$$

Here m_A and A_S are the mass and the external surface area of the adsorbent, respectively; V_L is the liquid phase volume.

By combining Eqs. 8 and 10, considering that $\rho_S = m_A/V_A$ (V_A = adsorbent volume), we finally get the *LDF* equation:

$$\frac{dq}{dt} = k_D(q_s - q) \tag{11}$$

$$k_D = \frac{A_S}{V_A}k_s \tag{12}$$

Here k_D is the *LDF* mass transfer coefficient.

Equation 11 has been largely used for studying gas adsorption [24–26] and, to a lesser extent, adsorption from aqueous solutions [27, 28]. The applicability of Eq. 11 to experimental data depends on the specific isotherm describing the adsorption equilibrium at the outer surface of the particle. When the latter equilibrium is described by a linear isotherm, the adsorbed equilibrium amount at the outer surface, q_s, is given by:

$$q_s = KC \tag{13}$$

Here K is the linear adsorption equilibrium constant and C is the solute concentration in equilibrium with q_s.

Substitution of Eq. 13 into 11 produces, after integration [29]:

$$q = \frac{C_0 K}{1 + KX}(1 - \exp(-(1 + KX)k_D t)) \tag{14}$$

Here C_0 is the solute concentration at $t = 0$, X is the adsorbent dosage (m_A/V_L).

The simplistic approach of Eq. 14 may be improved and extended by assuming a non-linear relationship between the surface and the liquid phase concentration at equilibrium.

This work examines the case where the equilibrium is described by the Langmuir model. An exact analytical solution of the resulting Langmuir-based linear driving force equation (*LLDF*) is derived and discussed. The derived equation is tested for its effectiveness to fit the adsorption kinetic data of the chemical compound boscalid

onto a high-porosity granular activated carbon (*GAC*). Boscalid, a carboxamide fungicide, was selected for this work, because is an understudied emerging water pollutant [6, 30–32]. In 2009, during a monitoring campaign of USA surface water and groundwater, it was detected more frequently than atrazine and metolachlor, two herbicides that are typically the most frequently occurring pesticides in many large-scale water quality studies [33].

Model derivation

Let us assume that (i) a rapid equilibrium (pre-equilibrium hypothesis) is established between the solute in solution and the adsorbate located at the outer surface of the adsorbent, and that (ii) this equilibrium is described by the Langmuir isotherm. It follows that q_s can be expressed at any time by:

$$q_s = \frac{q_m K_L C}{1 + K_L C} \tag{15}$$

Here q_m and K_L are the maximum adsorption capacity of the adsorbent and the Langmuir equilibrium constant, respectively, whereas C the solute concentration in equilibrium with q_s.

If the adsorbing substance is initially present only in the liquid phase, the adsorption amount q at any time is given by:

$$q = \frac{C_0 - C}{X} \tag{16}$$

Here C_0 and X are the initial solute concentration and the adsorbent dosage, respectively.

Substituting Eqs. 15 and 16 into Eq. 11 gives a formulation of the *LDF* model in terms of liquid phase concentration (C) instead of q:

$$\frac{dC}{dt} = -Xk_D\left(\frac{q_m K_L C}{1 + K_L C} - \frac{C_0 - C}{X}\right) \tag{17}$$

or

$$\frac{dC}{dt} = -K_L k_D\left(\frac{C^2 + \left(q_m X - C_0 + \frac{1}{K_L}\right)C - \frac{C_0}{K_L}}{1 + K_L C}\right) \tag{18}$$

By rearranging and separating the variables, we get:

$$\frac{K_L C + 1}{C^2 + \left(q_m X - C_0 + \frac{1}{K_L}\right)C - \frac{C_0}{K_L}}dC = -K_L k_D dt \tag{19}$$

Using the partial fraction method [34], Eq. 19 can be integrated for the boundary conditions, $C = C_0$ at $t = 0$ and $C = C$ for $t = t$, leading to:

$$\left(K_L - \frac{1 + K_L C_2}{C_2 - C_1}\right) \ln \frac{C - C_1}{C_0 - C_1} + \frac{1 + K_L C_2}{C_2 - C_1} \ln \frac{C - C_2}{C_0 - C_2} = -K_L k_D t \tag{20}$$

Here C_1 and C_2 denote the roots of the polynomial in the denominator of Eq. 19.

By inspecting Eq. 18, one observes that the equilibrium conditions, i.e. $dC/dt = 0$, are satisfied when the numerator on the right side equals zero, implying that the solute concentration at equilibrium, C_e, is one of the roots of the polynomial (e.g. C_1):

$$C_1 = C_e \tag{21}$$

Furthermore, from Eq. 16, we have that

$$C_e = C_0 - q_e X \tag{22}$$

$$C_2 = C_0 - q_2 X \tag{23}$$

Here q_e and q_2 are the adsorbate concentration associated with C_e and C_2, respectively.

Therefore, by substituting Eqs. 16 and 21–23 into Eq. 20, and after rearranging, we obtain:

$$\ln \frac{(q_e - q)}{q_e} + \frac{q_e - q_m}{q_e - q_2} \ln \frac{(q_2 - q)}{(q_e - q)} \frac{q_e}{q_2} = -k_D t \tag{24}$$

This is an exact solution of the Langmuir-based Liner Driving Force model (*LLDF*). Here q_2 is given by [34]:

$$q_2 = \frac{q_m}{q_e} \frac{C_0}{X} \tag{25}$$

It is interesting to note that from the definition of q_e, q_2 and q_m, we get the following inequality:

$$q_e \leq q_m \leq q_2 \tag{26}$$

Equation 26 permits us to identify two suitable conditions under which the *LLDF* model reduces to the so-called pseudo-first order (*PFO*) model widely used in adsorption studies [35–38]:

$$q = q_e(1 - \exp(-k_1 t)) \tag{27}$$

Here k_1 is the *PFO* kinetic rate constant.

$$1)\ q_2 > > q \tag{28}$$

Under this condition, Eq. 24 reduces to:

$$\ln\frac{(q_e-q)}{q_e}+\frac{q_e-q_m}{q_e-q_2}\ln\frac{q_e}{(q_e-q)}\approx -k_D t \tag{29}$$

When this is solved for q, it gives the *PFO* equation

$$q=q_e\left(1-\exp\left(-k_{1,1}t\right)\right) \tag{30}$$

Here the kinetic rate constant $k_{1,1}$ is equal to:

$$k_{1,1}=\frac{q_e-q_2}{q_m-q_2}k_D \tag{31}$$

$$2)\ q_e\cong q_m \tag{32}$$

Under this condition, Eq. 24 reduces to:

$$q=q_e(1-\exp(-k_D t)) \tag{33}$$

Equation 33 suggests that the *LLDF* model is well approximated by the *PFO* model (with kinetic rate constant k_D) when the adsorbate concentration at equilibrium is close to the maximum adsorption capacity of the adsorbent (e.g. at very high initial solute concentration, C_0).

Materials and methods

Materials

Boscalid and all other reagents were purchased from Sigma-Aldrich.

The granular activated carbon (GAC) used for the adsorption experiments was provided by Chemviron Carbon (UK). The GAC particle size ranged 1–2 mm, and the BET surface area was 774 m^2/g. Further details on GAC composition are reported elsewhere [20].

Adsorption experiments

Adsorption measurements were performed at 25 °C by batch experiments. Twenty millilitres of boscalid aqueous solution with concentration ranging from 1 to 4.0 mg L^{-1} were put into polypropylene tubes with 5 mg of GAC. The samples were stirred at 60–210 rpm on an orbital shaker till the equilibrium was attained (8 days). At programmed times (from 1 min to 8 days after the onset of the experiments), small aliquots of the supernatant were collected and analysed by HPLC. HPLC measurements were performed on a chromatographic Waters system consisting of a 515 HPLC Pump and a 2487 dual λ absorbance detector, equipped with a C18 reversed-phase column TC-18(2) Agilent (4.6 × 250 mm). Boscalid was eluted by a $CH_3CN(60\%)/H_2O(40\%)$ isocratic method with a flow rate of 1 mL min^{-1} and detected at the wavelength of 260 nm. Boscalid adsorption was

estimated by mass balance analysis, by comparing its concentration in solution before and after contact with GAC.

Results and discussion

Effect of agitation speed on the rate of adsorption

As mentioned in the introductory section, the rate of disappearance of the solute from the solution in the presence of porous media is predominantly governed by film diffusion and intraparticle diffusion. In order to apply the *LLDF* model, film diffusion contribution must be negligible. An increase in the agitation speed reduces the bounding layer surrounding the adsorbent particle, thus shortening the "film diffusion" step. As expected, increasing the agitation speed (rpm) significantly enhanced the initial reaction rate v_0 (Fig. 1). Interestingly, the increase in the adsorption rate declined progressively with rising agitation speed and stabilized at rpm $\geq$ 190; at this point, film diffusion was no longer relevant and intraparticle diffusion became the sole rate-controlling step of the adsorption process. Based on these results, an agitation speed of 210 rpm was chosen for kinetic experiments.

Application of the *LLDF* model

Equation 24 contains three unknown parameters, namely q_m, q_e and k_D. The simultaneous estimation of these parameters can be obtained only by implicit least-squares method (e.g. by using Origin® 9.0 software), since Eq. 24 is not invertible with respect to q. Alternatively, one can preliminarily determine q_m and q_e from the adsorption isotherm and then apply Eq. 24 for estimating k_D. In this work, the latter method was chosen for analysing the adsorption data of boscalid onto GAC.

Fig. 2 shows the adsorption kinetics of boscalid onto GAC at different initial solute concentrations.

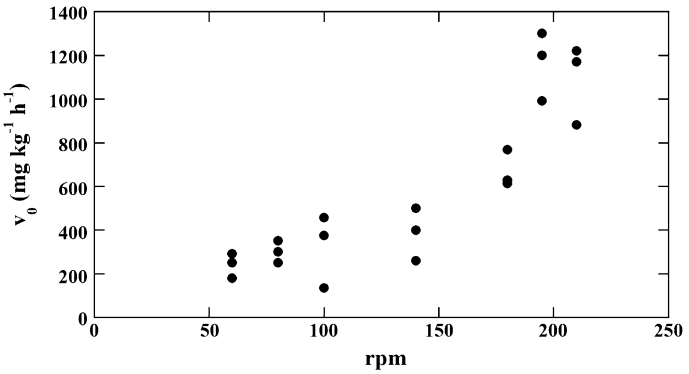

Fig. 1 Dependence of the initial adsorption rate (v_0) on the agitation speed (*rpm*); initial boscalid aqueous concentration = 3 mg L^{-1}; adsorbent dosage = 20 mg L^{-1}

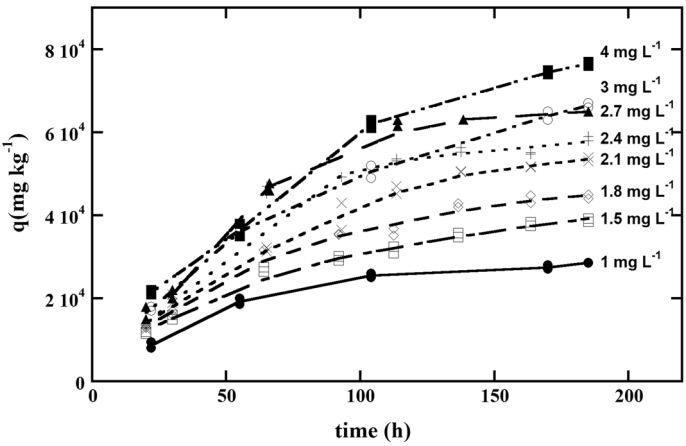

Fig. 2 Adsorption kinetics of boscalid onto GAC at different initial aqueous concentrations; agitation speed = 210 rpm; adsorbent dosage = 20 mg L^{-1}

As can be seen, after an initial phase of fast uptake, the adsorption process gradually declined until the equilibrium was reached (within 8 days for all the experimental conditions tested). The adsorption amount values at equilibrium (q_e) were plotted against C_e (Fig. 3) and fitted by the Langmuir model (Eq. 15) for determining the adsorption isotherm parameters K_L and q_m. The results of the fitting procedure were satisfactory, as inferred from the high value of R^2 and the moderate low errors associated with K_L and q_m (Table 1), suggesting that the Langmuir model adequately describes the adsorption equilibrium of boscalid onto GAC.

The values obtained for K_L and q_m were used to calculate, for each q value reported in Fig. 2, the left side of Eq. 24 (hereafter referred as LS_{LLDF}), and the entire data set generated by this procedure was merged and plotted against t (Fig. 4).

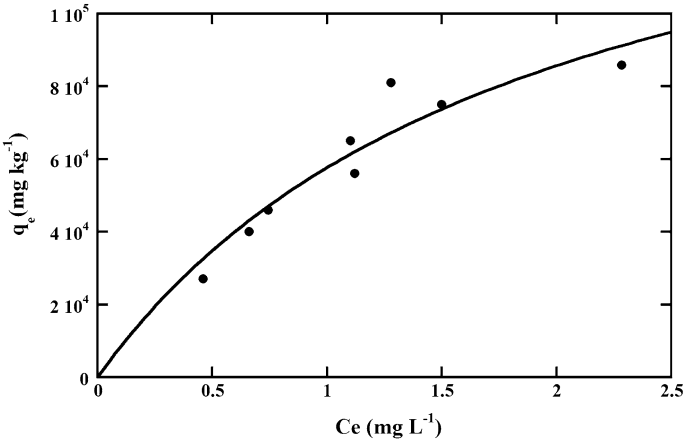

Fig. 3 Adsorption isotherm of boscalid onto GAC; T = 25 °C

Table 1 Equilibrium and kinetic parameters of boscalid adsorption onto GAC

Langmuir isotherm			LLDF model		Langmuir kinetics	
K_L (L mg^{-1})	q_m (mg g^{-1})	R^2	k_D (h^{-1})	R^2	k_a (L mg^{-1} h^{-1})	R^2
0.53 ± 0.22	167 ± 41	0.89817	0.0084 ± 0.0001	0.96409	0.84777 ± 0.00005	0.84777

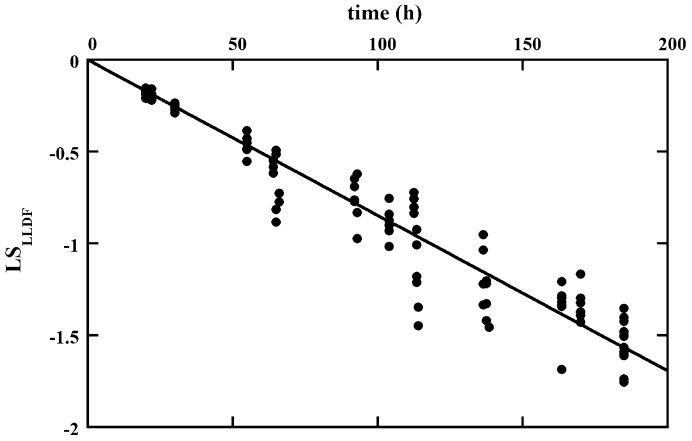

Fig. 4 Plot of LS_{LLDF} versus time using the theoretical values of q_e as determined by the Langmuir isotherm; K_L = 0.53, q_m = 167 mg g^{-1}

According to Eq. 24, a plot of LS_{LLDF} vs t should produce a straight line with slope $-k_D$. The fair linear correlation between LS_{LLDF} and t (Fig. 4) suggests that the *LLDF* model is suitable for modelling the adsorption kinetics of boscalid onto GAC. The value of k_D, determined from the slope of the line in figure, was 0.0084 h^{-1}. In line with former work [20], these results suggest that adsorption onto GAC is mainly controlled by diffusion processes due to the high porosity of this material. In order to verify this hypothesis, the kinetic experimental data were fitted with the integrated Langmuir kinetic model [34], rearranged in the following form:

$$\frac{1}{(q_2 - q_e)X} \ln\left(\frac{1 - \frac{q}{q_e}}{1 - \frac{q}{q_2}}\right) = -k_a t \tag{34}$$

Here k_a is the microscopic adsorption rate constant. The Langmuir kinetic model assumes that the rate of adsorption is not diffusion-limited. If this assumption were valid, the left side of Eq. 34 (denoted by LS_{Lang} in Fig. 5) should be linearly correlated to t, with a slope = $-k_a$. Fig. 5 shows the application of Eq. 34 to the experimental data.

As can be seen, the Langmuir kinetic model gives less satisfactory results compared to the *LLDF* model because data points are more scattered (see also R^2 values in Table 1), especially at late reaction time, resulting in a poorer description of the adsorption kinetic profiles (see, as an example, Fig. 6). This reinforces the

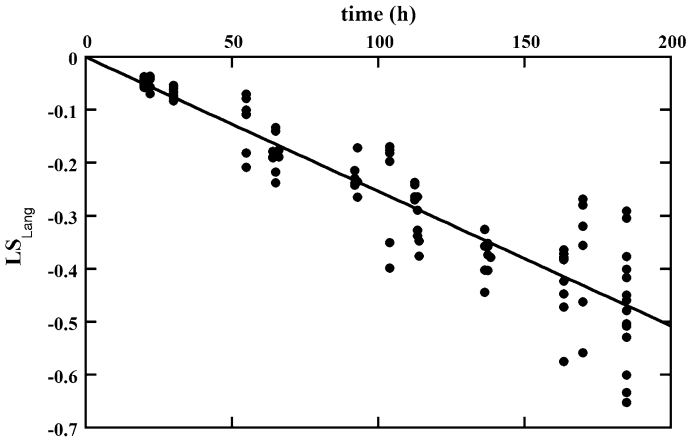

Fig. 5 Plot of LS_{Lang} against time using the theoretical values of q_e as determined by the Langmuir isotherm; $K_L = 0.53$, $q_m = 167$ mg g^{-1}

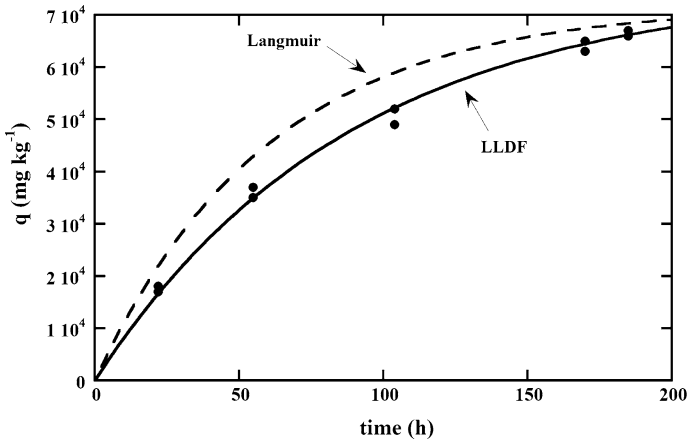

Fig. 6 Comparison between experimental adsorption data (filled circles) and theoretical data based on *LLDF* (solid line) and Langmuir kinetic (dashed line) models, respectively; initial boscalid aqueous concentration = 3 mg L^{-1}; adsorbent dosage = 20 mg L^{-1}

hypothesis that the adsorption of boscalid onto GAC is governed by pore diffusion and not by surface reaction.

Conclusions

A simple Langmuir-based equation (*LLDF*) can be derived from the *LDF* model and successfully applied to modelling experimental kinetics data from the adsorption of boscalid onto *GAC*. The *LLDF* model depends on three unknown parameters, namely the adsorbed amount at equilibrium (q_e), the maximum adsorbent capacity (q_m) and the mass transfer coefficient (k_D).

The applicability of the *LLDF* model can be verified from the linearity of the plot of *LS(t)* against *t*.

References

1. Smirnov IYu, Levin VN, Zdyumaeva NP (2004) Protein adsorption on erythrocytic membranes and its effect on erythrocyte rheology in athletes during competition exercise. Hum Physiol 30(3):364–368
2. Yin G, Janson JC, Liu Z (2000) Characterization of protein adsorption on membrane surface by enzyme linked immunoassay. J Membr Sci 178(1–2):99–105
3. Fernandes MC, Cox L, Hermosín MC, Cornejo J (2003) Adsorption–desorption of metalaxyl as affecting dissipation and leaching in soils: role of mineral and organic components. Pest Manag Sci 59:545–552
4. Gimsing AL, Borggaard OK, Bang M (2004) Influence of soil composition on adsorption of glyphosate and phosphate by contrasting Danish surface soils. Eur J Soil Sci 55:183–191
5. Liu XG, Dong FS, Xu J, Yuan SK, Zheng YQ (2014) Dissipation and adsorption behavior of the insecticide ethiprole on various cultivated soils in China. J Integr Agr 13(11):2471–2478
6. Salvestrini S, Canzano S, Iovino P, Leone V, Capasso S (2014) Modelling the biphasic sorption of simazine, imidacloprid, and boscalid in water/soil systems. J Environ Sci Heal Part B 49:578–590
7. Akhtar J, Amin NAS, Shahzad K (2016) A review on removal of pharmaceuticals from water by adsorption. Desalin Water Treat 57(27):12842–12860
8. Bhatnagar A, Kumar E, Sillanpää M (2011) Fluoride removal from water by adsorption—a review. Chem Eng J 171(3):811–840
9. Howarth AJ, Katz MJ, Wang TC, Platero-Prats AE, Chapman KW, Hupp JT, Farha OK (2015) High efficiency adsorption and removal of selenate and selenite from water using metal-organic frameworks. J Am Chem Soc 137(23):7488–7494
10. Salvestrini S, Jovanović J, Adnadjević B (2016) Comparison of adsorbent materials for herbicide diuron removal from water. Desalin Water Treat 57(48–49):22868–22877
11. Suresh S, Sundaramoorthy S (2014) Green chemical engineering. An introduction to catalysis, kinetics, and chemical processes. CRC Press, Boca Raton
12. Faust SD, Aly OM (1998) Chemistry of water treatment. CRC Press, Boca Raton. ISBN 9781575040110
13. Fick A (1855) Ueber diffusion. Ann Phys 170(1):59–86
14. Lente G (2015) Deterministic kinetics in chemistry and systems biology. Springer, Berlin. ISBN 978-3-319-15482-4
15. Cranck J (1975) The mathematics of diffusion. Claredon Press, Oxford
16. Weber WJ, Morris JC (1963) Kinetics of adsorption on carbon from solution. J Sanit Eng Div ASCE 89:31–59
17. León G, García F, Miguel B, Bayo J (2016) Equilibrium, kinetic and thermodynamic studies of methyl orange removal by adsorption onto granular activated carbon. Desalin Water Treat 57(36):17104–17117
18. Lu X, Shao Y, Gao N, Ding L (2015) Equilibrium, thermodynamic, and kinetic studies of the adsorption of 2,4-dichlorophenoxyacetic acid from aqueous solution by MIEX resin. J Chem Eng Data 60:1259–1269
19. Omri A, Wali A, Benzina M (2016) Adsorption of bentazon on activated carbon prepared from *Lawsonia inermis* wood: equilibrium, kinetic and thermodynamic studies. Arab J Chem 9:1729–1739
20. Salvestrini S, Vanore P, Bogush A, Mayadevi S, Campos LC (2017) Sorption of metaldehyde using granular activated carbon. J Water Reuse Desalin 7(3):280–287
21. Wu FC, Tseng RL, Juang RS (2009) Initial behavior of intraparticle diffusion model used in the description of adsorption kinetics. Chem Eng J 153:1–8
22. Bonzel HP (2001) Adsorption on surfaces and surface diffusion of adsorbates. Springer, Berlin
23. Glueckauf E, Coates JI (1947) Theory of chromatography. Pt. 4. The influence of incomplete equilibrium on the front boundary of chromatograms and the effectiveness of separation. J Chem Soc 149(2):1315–1321

24. Chauveau R, Grévillot G, Marsteau S, Vallières C (2013) Values of the mass transfer coefficient of the linear driving force model for VOC adsorption on activated carbons. Chem Eng Res Des 91(5):955–962
25. Simo M, Sivashanmugam S, Brown CJ, Hlavacek V (2009) Adsorption/desorption of water and ethanol on 3A zeolite in near-adiabatic fixed bed. Ind Eng Chem Res 48(20):9247–9260
26. Xiao G, Singh R, Chaffee A, Webley P (2011) Advanced adsorbents based on MgO and K_2CO_3 for capture of CO_2 at elevated temperatures. Int J Greenh Gas Control 5(4):634–639
27. Acar ET, Ortaboy S, Atun G (2015) Adsorptive removal of thiazine dyes from aqueous solutions by oil shale and its oil processing residues: characterization, equilibrium, kinetics and modeling studies. Chem Eng J 276:340–348
28. Schuricht F, Borovinskaya ES, Reschetilowski W (2017) Removal of perfluorinated surfactants from wastewater by adsorption and ion exchange—influence of material properties, sorption mechanism and modelling. J Environ Sci 54:160–170
29. Worch E (2012) Adsorption technology in water treatment. Walter de Gruyter GmbH & Co. KG, Berlin. ISBN 978-3-11-024022-1
30. Ahrens L, Daneshvar A, Lau AE, Kreuger J (2015) Characterization of five passive sampling devices for monitoring of pesticides in water. J Chromatogr A 1405:1–11
31. Salvestrini S, Vanore P, Iovino P, Leone V, Capasso S (2015) Adsorption of simazine and boscalid onto acid-activated natural clinoptilolite. Environ Eng Manag J 14:1705–1712
32. Zou N, Yuan C, Chen R, Yang J, Li Y, Li X, Pan C (2017) Study on mobility, distribution and rapid ion mobility spectrometry detection of seven pesticide residues in cucumber, apple, and cherry tomato. J Agric Food Chem 65:182–189
33. Reilly TJ, Smalling KL, Orlando JL, Kuivila KM (2012) Occurrence of boscalid and other selected fungicides in surface water and groundwater in three targeted use areas in the United States. Chemosphere 89:228–234
34. Salvestrini S (2018) Analysis of the Langmuir rate equation in its differential and integrated form for adsorption processes and a comparison with the pseudo first and pseudo second order models. Reac Kinet Mech Cat 123(2):455–472
35. Colella A, de Gennaro B, Salvestrini S, Colella C (2015) Surface interaction of humic acids with natural and synthetic phillipsite. J Porous Mater 22(2):501–509
36. Lagergren S (1898) Zur theorie der sogenannten adsorption gelöster stoffe. K Sven Vetenskapsakad Handl 24(4):1–39
37. Lee CR, Kim HS, Jang IH, Im JH, Park NG (2011) Pseudo first-order adsorption kinetics of N719 dye on TiO2 surface. Appl Mater Interfaces 3(6):1953–1957
38. Tseng RL, Wu FC, Juang RS (2010) Characteristics and applications of the Lagergren's first-order equation for adsorption kinetics. J Taiwan Inst Chem E 41(6):661–669